J Sol-Gel Sci Technol (2009) 51:10–22
DOI 10.1007/s10971-009-1988-0

ORIGINAL PAPER

# The molecular composition of non-modified and acac-modified propoxide and butoxide precursors of zirconium and hafnium dioxides

**Gerald I. Spijksma · Gulaim A. Seisenbaeva · Andreas Fischer · Henny J. M. Bouwmeester · Dave H. A. Blank · Vadim G. Kessler**

Received: 20 November 2008 / Accepted: 29 April 2009 / Published online: 19 May 2009


**Abstract** Long-term storage at 0 °C of a paraffin-sealed flask with commercial 70 wt% solution of zirconium *n*-propoxide in *n*-propanol resulted in crystallization of an individual oxoalkoxide complex $Zr_4O(O^nPr)_{14}(^nPrOH)_2$ in over 20% yield. The structure of this molecule can be described as a triangular $Zr_3(\mu_3\text{-}O)(OR)_{10}(ROH)$ core of 3 edge-sharing octahedrons with an additional $Zr(OR)_4$ (ROH) unit attached through a pair of ($\mu$-OR) bridges. Mass spectrometric and $^1H$ NMR investigation of the commercial samples of the most broadly applied zirconium and hafnium n-propoxides and *n*-butoxides indicate the presence of analogous species in the commercial alkoxide precursors. The content of oxo-alkoxide species in the commercial precursors has been estimated to be ~20% for *n*-propoxide and ~35% for zirconium *n*-butoxide. A new route has been presented for synthesis of the individual crystalline mixed ligand precursor $[Zr(O^nPr)(O^iPr)_3(^iPrOH)]_2$, from zirconium *n*-propoxide. A high yield has been observed (~90%), indicative of an almost complete precursor transformation. Mass spectrometry has shown that the synthesized mixed ligand precursor is dimeric, which makes it an attractive alternative to zirconium *n*-propoxide. Addition of 1 eq of Acetylacetone to zirconium or hafnium alkoxide precursors results in formation of dimeric $[M(OR)_3(acac)]_2$ in high yields. These species have limited stability (much higher for Hf than for Zr) and transform in solution into hydrolysis-insensitive $M(acac)_4$ through very unstable $M(acac)_3(OR)$ intermediates containing 7-coordinated metal centers. This transformation can be followed kinetically in hydrocarbon solvents by $^1H$ NMR and is noticeably accelerated by addition of parent alcohols. The obtained results clearly reveal limited applicability of EXAFS and XANES techniques for the study of such systems, especially in the context of structure prediction.

**Keywords** Precursor chemistry · Zirconium propoxide · Zirconium butoxide · Mass spectrometry · Sol–gel of $ZrO_2$ and $HfO_2$ · NMR · EXAFS · XANES · MTSAL concept

**Electronic supplementary material** The online version of this article (doi:10.1007/s10971-009-1988-0) contains supplementary material, which is available to authorized users.

G. I. Spijksma · H. J. M. Bouwmeester · D. H. A. Blank
Inorganic Materials Science, Faculty of Science & Technology, University of Twente, P.O. Box 217, 7500 AE Enschede, The Netherlands

G. I. Spijksma
e-mail: G.I.Spijksma@utwente.nl

G. I. Spijksma · H. J. M. Bouwmeester · D. H. A. Blank
MESA+ Institute for Nanotechnology, University of Twente, P.O. Box 217, 7500 AE Enschede, The Netherlands

G. I. Spijksma · G. A. Seisenbaeva · V. G. Kessler (✉)
Department of Chemistry, SLU, Box 7015, 750 07 Uppsala, Sweden
e-mail: Vadim.Kessler@kemi.slu.se

A. Fischer
Inorganic Chemistry, Royal University of Technology, 100 44 Stockholm, Sweden

## 1 Introduction

The alkoxides of zirconium and more recently, hafnium became widely used as precursors in preparation of oxide materials for various applications, ranging from porous membranes [1–3] and matrices in catalysis [4, 5] to dense dielectric and ferroelectric films in electronics [6, 7].

Despite the broad application of these alkoxide complexes, their molecular nature is not understood so far. Based on the current knowledge, none of the commercially available homometallic compounds can be considered as an ideal precursor. The cheap *n*-propoxide, "$Zr(O^nPr)_4$", at room temperature is a moisture-sensitive waxy solid [8]. It is delivered commercially in the form of 70 wt% solution in $^n$PrOH, of which the structural composition has been unknown. In an attempt to purify the precursor, Day et al. [8] obtained three different fractions upon vacuum distillation and could isolate crystals of a tetrameric species $Zr_4(OR)_{16}$ from one of these fractions. Analogously, zirconium *n*-butoxide is commercially available in a 80 wt% solution in $^n$BuOH. According to data of mass spectrometry presented by Turevskaya et al. [9], the main compound there is also $Zr_4(OR)_{16}$, i.e., similar to that in commercial zirconium *n*-propoxide. The structures of the species present in solutions of both zirconium and hafnium butoxides have recently been a topic of intensive studies applying X-ray absorption spectroscopy, EXAFS and XANES [10–12]. It is very interesting that for one and the same compound, $Zr(O^nBu)_4$, in a variety of solvents (toluene, alcohol, and mixtures of toluene and alcohol) and with apparently analogous raw data presented in the papers, Kanazhevskii et al. [10] and Bauer et al. [11] came to completely different models: Kolomiichuk et al. [10] described the molecule as an asymmetric tetramer with 4 types of Zr–Zr distances at 3.25–3.30, 3.47–3.50, 3.84, and 4.80 Å [10], while Bauer et al. concluded it to be a symmetric trimer with Zr–Zr distance of 3.56 Å [11]. It should be mentioned that the model in [10] was of much higher quality than in [11], Debye–Waller factors of about 0.003 compared to 0.06–0.11(!). Bauer et al. [11] also have some unclear reason directly ruled out the most common for triangular alkoxide cores structure motive including the trinuclear $M_3(\mu_3\text{-}O)$ core. This core was proposed by Caughlan [13] for a possible analog—the titanium ethoxide structure in solution. In making this decision the authors of [11] appealed to [14], where this structure has unfortunately not even been mentioned.

The zirconium isopropoxide isopropanol solvate complex, $[Zr(O^iPr)_4(^iPrOH)]_2$ [15] is a more stable and structurally well-defined compound. This complex is rather expensive and at room temperature poorly soluble in its parent alcohol and toluene, which complicates its application.

A mixed-ligand alkoxide $[Zr(O^iPr)(O\text{-}neo\text{-}C_5H_{11})_3(HO\text{-}neoC_5H_{11})]_2$ has been reported by Boyle [16]. It is claimed to be an attractive precursor for MOCVD, but not for sol–gel preparations due to its costs and the fact that it cannot be used in its parent alcohol. Recently, a promising mixed ligand precursor, $[Zr(O^nPr)(O^iPr)_3(^iPrOH)]_2$ has been reported by Seisenbaeva et al. [17].

The structure and reactivity of precursors formed on modification of zirconium and hafnium alkoxides with most common modifying ligand, Acetylacetone, remained unknown until very recently. In our preliminary communication, we have reported briefly on the structure of the zirconium isopropoxo-acetylacetonates [18].

The present study is focused towards evaluation of the structural composition of commercially available zirconium and hafnium *n*-propoxide and zirconium *n*-butoxide precursors and on their transformation in solution on addition of acetylacetone. In addition, $[Zr(O^nPr)(O^iPr)_3(^iPrOH)]_2$ is prepared *via* an alternative synthesis. Its properties are compared with those of the homoleptic zirconium precursors.

## 2 Experimental

All manipulations were carried out in a dry nitrogen atmosphere using the Schlenk technique or a glove box. The 70 wt% solution of "$Zr(O^nPr)_4$" (Lot: S20269-054) and 80 wt% solution of "$Zr(O^nBu)_4$" were purchased from Aldrich. Isopropanol (Merck, p.a.) was purified by distillation over $Al(OPr)_3$ and toluene (Merck, p.a.) by distillation over $LiAlH_4$.

$^1$H NMR and 2-d NMR, using COSY and HSQC, spectra were recorded in $CDCl_3$ solutions on a Bruker 400 MHz spectrometer at 243 K. An additional control has been carried out with the same product from Alfa Aesar GMBH (044770 250 g LOT: E10Q01). The flask was opened in the dry box on the day of its arrival, and the comparative NMR study was made in a variable temperature regime (303–243 K) for $^1$H, $^{13}$C, and also for 2-dimensional pulse sequence for C–H correlation in heteronuclear single-quantum coherence (HSQS) mode. No $^{13}$C NMR spectra have been recorded for the compounds **2–4** in the view of their quick transformation in time (it would be impossible to provide a reliable explanation taking into account the relatively long duration of a conventional $^{13}$C experiment).

The FTIR study of the samples was carried out as nujol mulls using Perkin–Elmer Spectrum 100 instrument. The frequencies of C–H vibrations are for metal alkoxide and $\beta$-diketonate complexes dependent only on the nature of ligand [33], and thus no parallel experiments with halogenated solvent for mull preparation have been carried out.

Mass spectra were recorded using a JEOL JMS-SX/SX-102A spectrometer, applying electron beam ionization ($U = 70$ eV) with direct probe introduction. The results of microanalysis (C, H, N) were obtained by Mikrokemi AB, Uppsala, Sweden. In the view of poor stability of the compounds **2–4** in time, their purity was controlled by $^1$H NMR exclusively, because low temperature treatment used

on-site could not be guaranteed at the mentioned commercial facility.

## 2.1 Synthesis

### *2.1.1 Fractions of zirconium n-propoxide*

For NMR analysis, zirconium *n*-propoxide (~2 ml) was dried under vacuum (0.1 mm Hg) at room temperature, which resulted in a waxy yellow liquid, as described in ref. [8]. Also an amount of solid phase was obtained. Freshly prepared samples of both phases, i.e., the waxy yellow liquid and solid, were dissolved in $CDCl_3$ which was dried using zeolites, for NMR analysis. Element analysis and mass spectrometry were performed on the solid phase.

Samples of zirconium *n*-butoxide, both of the waxy yellow liquid and solid phase, were obtained and prepared in a corresponding manner. Both samples were analysed by $^1$H NMR. The solid phase was again examined by mass spectrometry.

Both according to a recently developed technique [17] and following a new synthesis route **[Zr(O$^n$Pr)(O$^i$Pr)$_3$ ($^i$PrOH)]$_2$** was prepared in the following way. The solvent of 10 ml of 70 wt% solution of "Zr(O$^n$Pr)$_4$" was removed under vacuum (0.1 mm Hg), and the product redissolved in 40 ml mixture of toluene/isopropanol (1:1 volume ratio). The solvent was removed by drying under vacuum (0.1 mm Hg). During the removal of the solvent, the first crystals appeared. Subsequently, 10 ml of isopropanol was added and the solution refluxed for 15 min. The sequence of redissolving, refluxing and removal of the solvent was repeated once. Then the dried product was dissolved in a 10 ml mixture of toluene and isopropanol (1:1 volume ratio) and upon slightly heating, a clear solution was obtained. After allowing the solution to stand over night at −30 °C, a large number of crystals were obtained. The solvent was removed from the crystals and concentrated by partial evaporation under vacuum (0.1 mm Hg). After addition of 3 ml of isopropanol, the solution was placed again for crystallization at −30 °C. The latter procedure was repeated up to a yield of over 90%. Found, %: C 45.9; H 9.5. Calc. For $C_{30}H_{72}O_{10}Zr_2$, %: C 46.5; H 9.4. IR, cm$^{-1}$: 3,156 m br, 1,365 w, 1,338 w, 1,160 s, 1,132 s, 1,081 w, 1,050 w, 1,015 s, 980 m, 953 m, 887 w, 844 m, 820 sh, 579 sh, 556 s, 521 m, 455 s, 431 m. NMR $^1$H $\delta$, ppm (interpretation): 5.9 singlet broad (2H, O*H*), 4.28 septet (8H, C*H*), 3.36 triplet (4H, C$H_2$), 1.65 sextet (4H, C$H_2$), 1.18 doublet (48H, $J_{C–H}$ = 6.1 Hz, C$H_3$, $^i$Pr), 0.87 triplet (6H, $J_{C–H}$ = 5.9 Hz, C$H_3$, $^n$Pr).

**Zr$_4$O(O$^n$Pr)$_{14}$($^n$PrOH)$_2$ (1)**. A portion of about 15 ml of the original 70 wt% zirconium propoxide solution in *n*-propanol was left in a fridge at 0° for over a 1-year period in a flask, sealed with melted paraffin. Huge (3–5 mm) poorly shaped transparent crystals precipitated on the bottom. The X-ray single crystal study (see below) identified it as Zr$_4$O(O$^n$Pr)$_{14}$($^n$PrOH)$_2$ (**1**). IR, cm$^{-1}$: 3,068 m br, 1,678 w br, 1,461 s, 1,437 sh, 1,380 s, 1,362 m, 1,297 w, 1,275 m, 1,252 m, 1,156 s br, 1,131 s, 1,072 s, 1,049 s, 1,004 s, 970 s, 909 w, 888 m, 863 m, 782 w, 754 w, 599 m, 550 s, 512 m, 464 s, 411 m. NMR $^1$H, $\delta$, ppm (interpretation): 4.00 unresolved (28H, $\alpha$-C$H_2$, OR) 3.63 triplet (4H, $\alpha$-C$H_2$, ROH), 1.71 not completely resolved sextet, (32H, $\beta$-C$H_2$), 0.82 overlapping triplets (48H, C$H_3$).

**[Zr(O$^i$Pr)$_3$(acac)]$_2$ (2)**. Zirconium isopropoxide solvate (weight: 3.78 g (9.8 mmol)) was dissolved in a 12 ml mixture of hexane and toluene (volume ratio 2:1). After adding an equivalent amount of acetylacetone (0.98 g, 9.8 mmol), the sample was dried under vacuum (0.1 mm Hg) and subsequently re-dissolved in 4 ml hexane. Crystallization occurred during cooling at −30 °C overnight. The solution was decanted from the obtained X-ray quality colorless crystals (4.02 g, yield 84%) that were identified as **2**. IR, cm$^{-1}$: 1,603 s, 1,525 s, 1,342 m, 1,307 sh, 1,276 m, 1,167 s br, 1,019 s, 980 w, 941 m br, 844 m, 820 m, 774 m, 657 m, 548 s br, 454 s, 427 s. NMR $^1$H $\delta$, ppm (interpretation): 5.44 sharp singlet (2H, C*H*-acac), 4.27 unresolved septet (6H, C*H*-$^i$Pr), 1.90 singlet (12H, C$H_3$-acac), 1.12 doublet (36H, $J_{C–H}$ = 6.1 Hz, C$H_3$-$^i$Pr). M–S, m/z(I, %), interpretation: 365(16.4), [Zr(acac)(O$^i$Pr)$_3$—H]$^+$, 307(100), [Zr(acac)(OPr)$_2$]$^+$.

**[Zr(O$^i$Pr)(acac)$_3$] (3)**. Zirconium isopropoxide solvate (weight: 0.79 g (2.05 mmol)) was dissolved in a 3 ml mixture of hexane and toluene (volume ratio 2:1). After the addition of two equivalent amounts of acetylacetone (0.41 g, 4.1 mmol), the sample was dried under vacuum (0.1 mm Hg) and subsequently re-dissolved in hexane. Crystallization occurred during cooling at −30 °C over night. The solution was decanted from the obtained X-ray quality crystals (0.45 g, yield 38%) that were identified as **3**. IR, cm$^{-1}$: 1,605 s, 1,527 s, 1,342 m, 1,307 sh, 1,276 m, 1,167 s br, 1,021 s, 978 w, 941 m br, 844 m, 820 m, 774 m, 657 m, 548 s br, 453 s, 429 s. NMR $^1$H: 5.54 singlet (3H, C*H*-acac), 4.19 septet (1H, C*H*-$^i$Pr), 1.96 singlet (18H, C$H_3$-acac), 0.94 unresolved dublet (6H, C$H_3$-$^i$Pr).

**[Hf(O$^i$Pr)$_3$(acac)]$_2$ (4)**. Hafnium isopropoxide solvate (weight: 1.41 g (3.0 mmol)) was dissolved in a 6 ml mixture of hexane and toluene (volume ratio 1:1). After addition of 0.30 g (3.0 mmol) of Hacac, i.e., 1 mol equivalent, the solution was removed from the mixture under vacuum (0.1 mm Hg). The obtained yellow, viscous liquid product was subsequently re-dissolved in 1 ml hexane. The sample was stored over night at −30 °C for crystallization. The solution was decanted from the obtained X-ray quality colorless crystals (1.15 g, yield 67%) that were identified as **4**. IR, cm$^{-1}$: 1,605 s, 1,527 s, 1,340 m, 1,309 sh, 1,275 m, 1,171 s br, 1,021 s, 981 w, 940

m br, 844 m, 820 m, 774 m, 660 m, 546 s br, 454 s, 429 s. NMR $^1$H $\delta$, ppm (interpretation): 5.63 sharp singlet (2H, C*H*-acac), 4.38 unresolved septet (6H, C*H*-$^i$Pr), 12.02 singlet (12H, C$H_3$-acac), 1.20 doublet (36H, $J_{C-H}$ = 6.0 Hz, C$H_3$-$^i$Pr).

#### 2.1.2 *Kinetic measurements*

A portion of freshly obtained crystals of $[M(O^iPr)_3(acac)]_2$, **2** or **4**, was dissolved in 2 ml of dry $CDCl_3$ to obtain the denoted concentration. A volume of 0.75 ml of the obtained solution was transferred immediately after dissolution into an NMR tube, placed then into in advance adjusted spectrometer. The measurement of the intensity of the $^1$H C*H*-acac signal started immediately afterwards. Figure 8 shows relative intensity of this signal disappearing in time, replaced by the arising signals, corresponding to $M(O^iPr)(acac)_3$ and $M(acac)_4$ species formed from them.

### 2.2 Crystallography

The data for compounds **1**–**4** were collected at room temperature (except for compound 1, where the data were collected also at 173 K) with SMART CCD 1 k diffractometer, using MoK$\alpha$-radiation (for details see Table 1). The structures were solved by direct methods. The metal atom coordinates were extracted from the initial solutions, while those of the other non-hydrogen atoms were located in subsequent difference Fourier syntheses. All non-hydrogen atoms were refined first in isotropic and then in anisotropic approximation. The coordinates of the hydrogen atoms were calculated geometrically using riding model and included into the final refinement in isotropic approximation. All calculations were performed using the SHELXTL-NT program package [19] on an IBM PC.

## 3 Results and discussion

### 3.1 Non-modified zirconium and hafnium alkoxides

The molecular composition of the zirconium and hafnium alkoxide precursors has been an object of intensive studies since the beginning of 1990s. The molecular structure of easily crystallizing and relatively sparingly soluble $[M(O^iPr)_4(^iPrOH)]_2$, M = Zr, Hf, has successfully been determined as a dimer with metal centers connected via a pair of alkoxy-bridging groups [15, 17, 20]. The stability of this structure was provided by the presence of two hydrogen bonds to solvating alcohol molecules, occupying a terminal axial position at each metal center (see Fig. 1d). Desolvation of these complexes on heating in vacuum resulted along with the solvent-free $M(O^iPr)_4$ in formation of oxo-impurities, symmetric triangular $M_3O(O^iPr)_{10}$ molecules, whose structure could unambiguously be identified with $^1$H NMR (see Fig. 1c) [9]. The X-ray single crystal data have been provided in literature for the zirconium oxo-tert-butoxide analog of these species [21].

The nature of the *n*-propoxide and *n*-butoxide derivatives applied much broader in the synthesis of materials turned to be much more difficult to establish. Day et al. [8] have carried out a complex separation procedure for the commercial 70 wt% $Zr(O^nPr)_4$ solution in $^n$PrOH based on vacuum distillation. They have concluded that the original material was definitely containing several fractions with different molecular properties. The product of repeated distillation crystallized as a waxy solid and was identified as $Zr_4(O^nPr)_{16}$. Its structure is depicted in Fig. 1a. Starting the present study we were expecting to find possibility to identify the possible oxo-alkoxide impurity and estimate its content in the industrial samples.

In fact, the oxo-impurity did crystallize spontaneously on prolonged storage at low temperature under strictly protecting conditions. The structure of this apparently major impurity in the $Zr(O^nPr)_4$ samples, the complex with $Zr_4O(O^nPr)_{14}(^nPrOH)_2$ (**1**) composition, is very interesting and illustrative (see Fig. 2): it contains a triangular $Zr_3$ ($\mu_3$-O) core, where the Zr atoms are connected also by 3 doubly bridging $\mu$-OR groups capping the three sides of the triangle. The coordination spheres of the two metal atoms Zr(2) and Zr(3) are completed in total by three alkoxide ligand and one solvating alcohol molecule, which is distributed statistically between positions O(11) and O(12) with a hydrogen bond between the groups in these two positions as a result. The coordination sphere for Zr(1) is completed by two bridging OR-groups shared with the additional zirconium center Zr(4). The latter is coordinated also to 3 terminal alkoxide ligands and the second solvating alcohol molecule in the composition of this complex. The coordination arrangement close to that of the zirconium atoms in the triangular core has been described for the hafnium atoms in $[Hf_3O(OEt)_{10}(EtOH)]_2$ [21], where 2 open triangular cores are connected via 2 pairs of alkoxide bridges. The hydroxyl group of the alcohol molecule attached to Zr(4), identified by O(13), is involved into hydrogen bonding to the tridentate oxo-ligand in the triangular $Zr_3(\mu_3$-O) unit. This additional hydrogen bonding stays apparently for the additional stabilization of the tetranuclear core of this molecule. This molecular structure provides also a perfect explanation for the contents of the mass spectra observed for the fractions separated on evacuation of the industrial samples of 70 wt% $Zr(O^nPr)_4$ solution in $^n$PrOH (see sect. "2" for the separation details). The solid state fraction is apparently enriched with the complex **1**, which results in a mass spectrum (see Table 2) with the fragmentation pattern based mainly on the more

**Table 1** Crystal data and the diffraction experiments details for compounds **1–4**

| | **1** | **2** | **3** | **4** |
|---|---|---|---|---|
| Chemical composition | $C_{42}H_{114}O_{17}Zr_4$ | $C_{28}H_{56}O_{10}Zr_2$ | $C_{18}H_{28}O_7Zr$ | $C_{28}H_{56}O_{10}Hf_2$ |
| Formula weight | 1256.21 | 735.17 | 447.62 | 909.71 |
| Crystal system | Monoclinic | Triclinic | Orthorhombic | Triclinic |
| Space group | P2(1)/n | P-1 | Pna2(1) | P-1 |
| $a$ (Å) | 12.0240(8) | 10.004(16) | 8.5444(17) | 9.497(5) |
| $b$ (Å) | 39.184(5) | 10.686(14) | 30.933(6) | 10.257(5) |
| $c$ (Å) | 14.4300(19) | 12.270(19) | 8.2339(16) | 11.388(6) |
| $\alpha$ (°) | 90 | 87.74(4) | 90 | 88.118(10) |
| $\beta$ (°) | 102.550(7) | 67.16(3) | 90 | 68.849(10) |
| $\gamma$ (°) | 90 | 64.75(5) | 90 | 64.744(9) |
| $V$ (Å$^3$) | 6636.2(13) | 1,081(3) | 2176.3(7) | 926.0(8) |
| $T$ (K) | 173(2) | 295(2) | 295(2) | 295(2) |
| $Z$ | 4 | 1 | 4 | 1 |
| $h_{min}$–$h_{max}$ | −14 to 14 | −11 to 10 | −9 to 4 | −9 to 9 |
| $k_{min}$–$k_{max}$ | −46 to 44 | −12 to 12 | −34 to 33 | −10 to 9 |
| $l_{min}$–$l_{max}$ | −17 to 16 | −14 to 14 | −7 to 9 | −10 to 11 |
| Theta (min–max) | 4.51–25.00 | 2.39–23.99 | 1.32–23.00 | 2.54–21.00 |
| Weighting details | $1/[s^2(Fo^2) + (0.0090P)^2 + 98.2508P]$ where $P = (Fo^2 + 2Fc^2)/3$ | $1/[s^2(Fo^2) + (0.0118P)^2 + 1.000P]$ where $P = (Fo^2 + 2Fc^2)/3$ | $1/[s^2(Fo^2) + (0.0563P)^2 + 10.000P]$ where $P = (Fo^2 + 2Fc^2)/3$ | $1/[s^2(Fo^2) + (0.0563P)^2 + 0.000P]$ where $P = (Fo^2 + 2Fc^2)/3$ |
| Number of independent reflections | 11,366 | 3,268 | 2,822 | 1,963 |
| Number of observed reflections | 7,831 [$I > 2$sigma($I$)] | 2,191 [$I > 2$sigma($I$)] | 2,092 [$I > 2$sigma($I$)] | 1,467 [$I > 2$sigma($I$)] |
| R1 | 0.0961 | 0.0448 | 0.0673 | 0.0502 |
| $w$R2 | 0.1844 | 0.0803 | 0.1418 | 0.1205 |

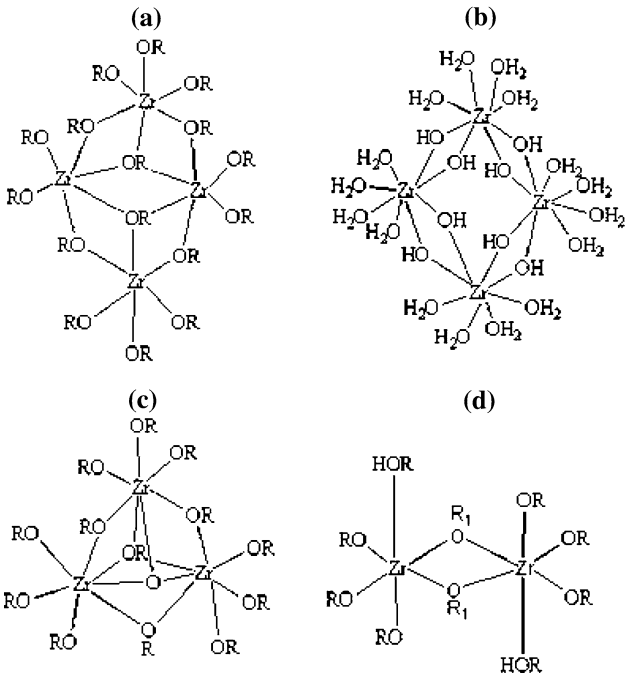


**Fig. 1** Schematic representation of $Zr_4(OPr)_{16}$ (**a**), $Zr_4(OH)_8(H_2O)_{16}^{8+}$ (**b**), $Zr_3O(OR)_{10}$ (**c**), and $[Zr(O^nPr)(O^iPr)_3(^iPrOH)]_2$ (**d**)

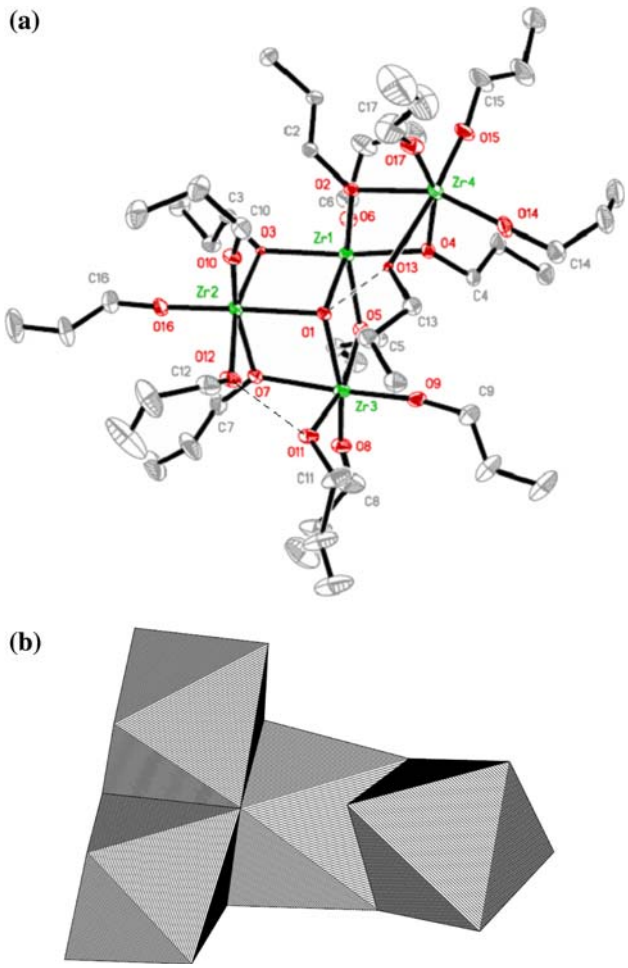


**Fig. 2** The molecular structure of $Zr_4O(O^nPr)_{14}(^nPrOH)_2$ as ORTEP-plot (**a**) and polyhedral plot (**b**)

thermally stable triangular $Zr_3(\mu_3\text{-O})$ unit together with minor fractions of tetranuclear oxo-fragments and considerable amounts of non-oxo dimeric and monomeric fragments, originating from both **1** (the part with Zr(4)) and the non-hydrolyzed zirconium propoxide. The liquid fraction is, in contrast, apparently enriched with the title compound, $Zr(O^nPr)_4$ and displays maximum of intensity (= highest gas phase content) for the ions $Zr(OR)_3^+$ (m/z = 267) and $Zr_2(OR)_6^+$ (m/z = 534).

Comparison of the $^1$H NMR spectra of the bulk sample of vacuum-dried 70 wt% $Zr(O^nPr)_4$ solution in $^n$PrOH with that of a single crystal of **1** (see Fig. 3) shows very distinct both common and different features: the broad signals at 4.00 and 3.63 ppm are present in the α-C$H_2$-region for both samples as well as a strong and broad signal at 1.71 ppm (β-C$H_2$). In addition, the bulk sample of "$Zr(O^nPr)_4$" contains two distinct signals at 3.86 and 3.73 ppm in the α-C$H_2$-region that can be attributed to the terminal and bridging groups in a $Zr_4(O^nPr)_{16}$ structure [8], respectively along with a signal at 1.48 ppm in the β-C$H_2$ region. In the spectrum of the solid fraction these additional signals have lower intensity, while in that of the liquid one they are dominating. Further confirmation of the attribution of the peaks can be found through comparison of the 2-dimensional COSY spectra for the solid fraction and the pure **1** (see Fig. 4).

Comparison of the integrated intensities between the spectra of the dried bulk sample and that for a $CDCl_3$ solution of a single crystal of **1** indicates that the latter constitutes over 20 wt% of the total of the alkoxide content in the commercial sample. These results have been confirmed by the variable temperature study of the fresh bulk sample of "$Zr(O^nPr)_4$" obtained from Alfa Aesar (see supplementary materials, Figs. FS1 and FS2): the better resolved low temperature signals permit to clearly trace compound **1** in the sample. In the Fig. FS1, it is possible to trace resolution of the C*H*-signals with decreasing temperature: the room temperature spectrum at 303 K displays only one type of signal for each n-propoxide functionality, α-C$H_2$, β-C$H_2$ and C$H_3$. Lowering of the temperature to 273 and then 243 K permits to distinguish at least 4 signals for each of those. The lowering of temperature itself is, however, clearly insufficient to reveal the complexity of the molecular composition of the samples. In the Fig. FS2, providing the HSQS analysis of C–H correlation at low temperature, it is possible to distinguish in fact 10 different signals for the α-C$H_2$ groups. One of them, corresponding to the solvating alcohol ($^{13}$C 64.66 ppm–1H 3.62 ppm) is rather week in the bulk sample, while another,

**Table 2** Interpretation of m/z(*I*) spectrum with ($Zr_3O(OR)_{10}$ = P; R = $^{n}Pr$)

| | | |
|---|---|---|
| 923 | (1.9) | $Zr_4O_2(OR)_9^+$ |
| 834 | (4.5) | $Zr_3O(OR)_9(OH)^+$, P–$C_3H_6$ |
| 817 | (9.0) | $Zr_3O(OR)_9^+$, P–OR |
| 792 | (0.6) | $Zr_3O(OR)_8(OH)_2^+$, P–$2C_3H_6$ |
| 715 | (18.5) | $Zr_3O_2(OR)_7^+$, P–OR–$R_2O$ |
| 690 | (2.2) | $Zr_3O_2(OR)_6(OH)_2^+$, P–$2C_3H_6$–2OR |
| 687 | (1.8) | $Zr_4O_2(OR)_5^+$ |
| 613 | (10.1) | $Zr_3O_3(OR)_5^+$, P–OR–$2R_2O$ |
| 593 | (3.5) | $Zr_2(OR)_7^+$ |
| 588 | (3.0) | $Zr_3O_3(OR)_4(OH)_2^+$, P–$2C_3H_6$–2OR–$R_2O$ |
| 586 | (3.5) | $Zr_4O_2(OR)_3(OH)^+$ |
| 548 | (17.8) | $Zr_2O(OR)_6^+$ |
| 544 | (28.4) | $Zr_4O_2(OR)_2(OH)_2^+$ |
| 539 | (10.5) | $Zr_3O(OR)_4(OH)^+$, P–$C_3H_6$–5OR |
| 534 | (10.5) | $Zr_2(OR)_6^+$ |
| 511 | (24.4) | $Zr_3O_4(OR)_3^+$, P–OR–$3R_2O$ |
| 491 | (100) | $Zr_2O(OR)_5^+$, P–OR–$Zr(OR)_4$ |
| 480 | (32.5) | $Zr_3O(OR)_3(OH)^+$, P–$C_3H_6$–6OR |
| 442 | (13.8) | $Zr_4O_3(OH)_2^+$ |
| 391 | (12.6) | $Zr_2(OR)_3(OH)_2^+$ |
| 267 | (20.5) | $Zr(OR)_3^+$ |
| 208 | (2.4) | $Zr(OR)_2^+$ |

corresponding apparently to a triply bridging alkoxide ligand ($^{13}C$ 63.00 ppm–1H 3.76 ppm), is missing in the solid fraction enriched with compound **1**. Estimation of their integral intensities provided basis for the quantitative evaluation.

It was of interest to see if analogous results could be obtained for zirconium *n*-butoxide. It turned out to be possible to obtain a solid and a waxy liquid phase. The data of $^{1}H$ NMR analysis of these phases show great similarity (Fig. 5) to that obtained for zirconium *n*-propoxide. The waxy liquid (Fig. 5a) again contains a number of unresolved peaks, while the spectra of the solid (Fig. 5b) contains the expected four signals for butoxide ligands and a signal (singlet) around 1.65 ppm indicating most probably the hydroxo-species present as an additional impurity in the original sample. The amount of the isolated phase, assumed to be $Zr_3O(OBu)_{10}$, is around 35% of the bulk as evaluated on the basis of the signal around 3.65 ppm. Mass spectrometry experiments were performed in order to get confirmation for the presence of $Zr_3O(OBu)_{10}$. Data of mass spectrometry presented by Turevskaya et al. [9] indicate that the majority of zirconium *n*-butoxide consists of $Zr_4(OR)_{16}$. The major fragment, $Zr_4O_3(OR)_9^+$ is found at 1,065 m/z (100%). In the spectrum obtained for the solid phase the major fragment is found at 628 m/z (100%) and assigned to $Zr_3O(OR)_9$. The signal at 1,065 m/z is <10%.

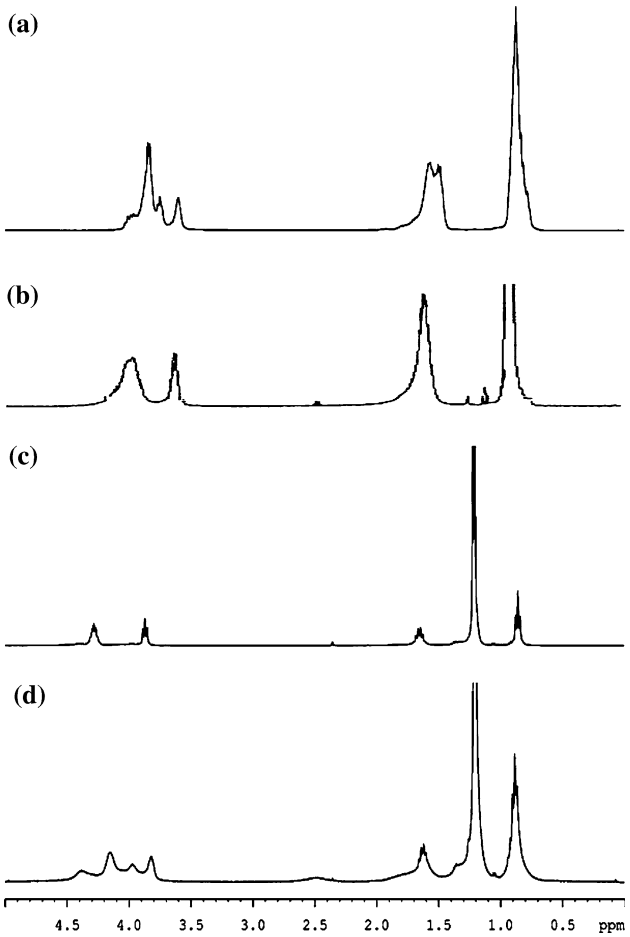


**Fig. 3** $^{1}H$ NMR spectra of the waxy liquid (bulk) phase of zirconium *n*-propoxide (**a**), and single crystals of $Zr_4O(O^{n}Pr)_{14}(^{n}PrOH)_2$ (**b**). The spectrum of $[Zr(O^{n}Pr)(O^{i}Pr)_3(^{i}PrOH)]_2$ is depicted in (**c**) and the residue of its synthesis in (**d**)

The great difference between the spectra of the solid and that of zirconium *n*-butoxide [9] indicates the presence of another compound. The presence of $Zr_3O(OR)_{10}$ in zirconium *n*-butoxide is demonstrated, since the NMR data (Fig. 5) is also in agreement with this compound (i.e., two partly overlapping triplets around 3.65 ppm in a ratio of 2:3 based on the intensity of the outer not overlapping signals). It is difficult to judge, however, whether the triangular $Zr_3O(OR)_{10}$ molecule is present as itself or coordinated further with one or several non-hydrolyzed alkoxide fragment as in compound **1**.

It has thus been demonstrated that in both zirconium *n*-propoxide and *n*-butoxide samples the compounds containing $Zr_3O(OR)_{10}$ cores are present. The commercially available products contain ~20 and ~35% of them, respectively. It is interesting to compare these data and the already available information about the molecular structures with the models proposed for zirconium and hafnium butoxide, on the basis of EXAFS data. In [11], it is

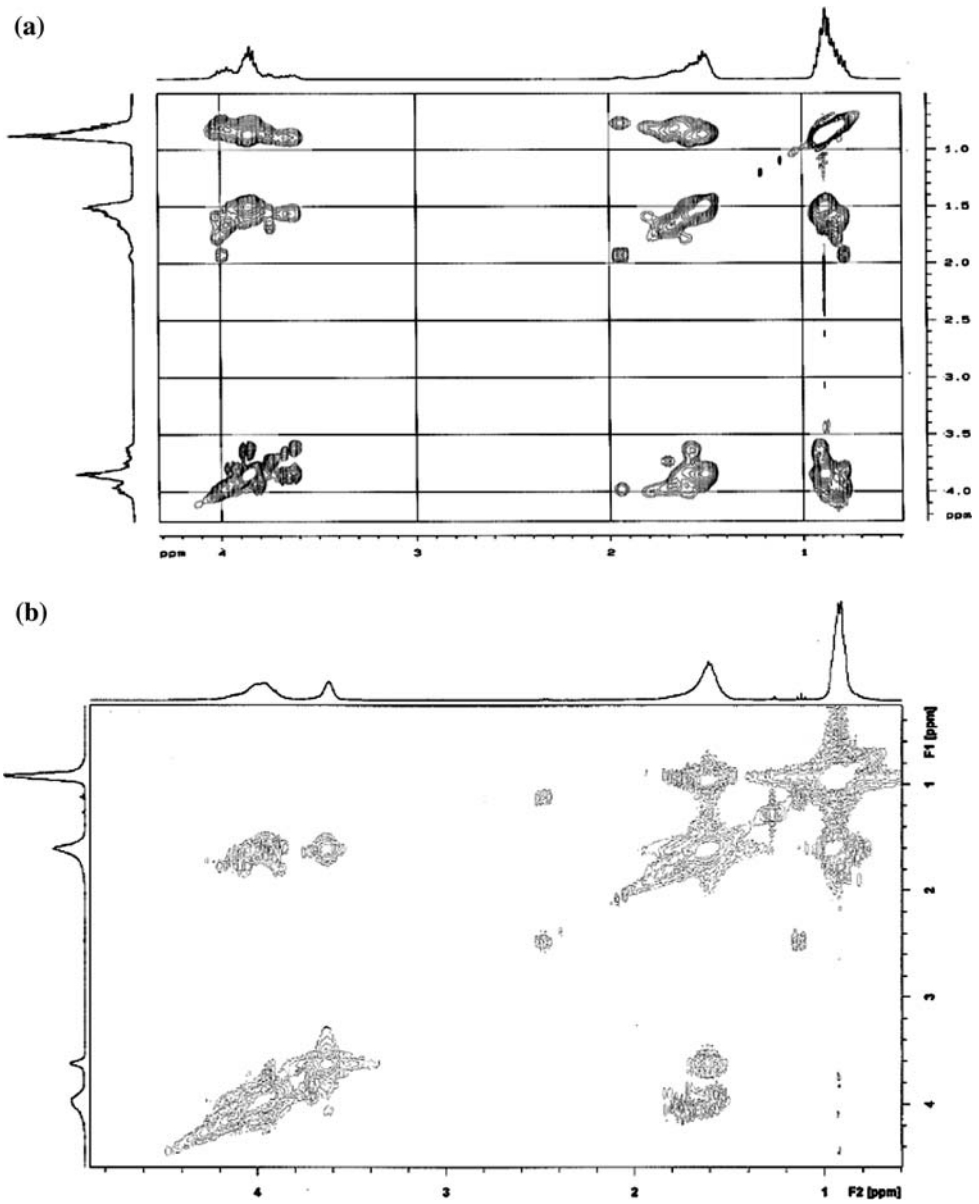


**Fig. 4** COSY spectra of the solid fraction of zirconium *n*-propoxide (**a**) and single crystals of $Zr_4O(O^nPr)_{14}(^nPrOH)_2$ (**b**)

postulated that only one type of Zr–Zr bond, corresponding to a dimer, 3.55–3.57 Å is present in the commercially available solutions of $Zr(O^nBu)_4$. In [10], the analogous radial distribution function was interpreted as manifestation of the presence of 4 types of distances: 3.27 Å (as in the $Zr_3O(O^tBu)_{10}$ trimer with 2 triply bridging ligands), 3.51 Å (intermediate between a trimer with only one triply bridging ligand of 3.45 Å as in **1** and a dimer with 2 doubly bridging alkoxide groups of 3.60 Å or a side of a square in a tetramer built up of octacoordinated centers such as in $Zr_4(OH)_8(H_2O)_{16}{}^{8+}$ core [21], see Fig. 1) and 2 longer ones, 3.84 and 4.80 Å, never observed in any reliable crystallographic model. This striking discrepancy results from the general problem summarized in [10] in the following way: "For the EXAFS method, as well as for other methods that demand simulation of experimental data, the number of independent parameters to be determined from experimental data is limited. For EXAFS, this number is $2\Delta k\Delta R/\pi$, where $\Delta k$ is the range of wave numbers in which experimental data are simulated; and $\Delta R$ is the range of distances in which the interatomic distances are determined. When the number of independent parameters is exceeded, the results of simulation become ambiguous".

The demonstrated presence of oxo-species should apparently effect application of the studied precursors in sol–gel process. The mechanism of metal alkoxide sol–gel is the thermodynamically driven micellar self-assembly [22], where the oxo-species should facilitate nucleation in the formation of the micelles. This can influence the size and concentration of the micelles. With the presence of

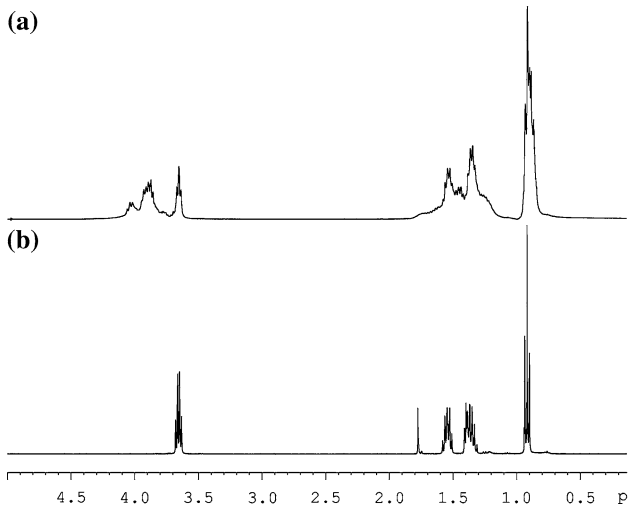


**Fig. 5** NMR spectra of the represents of the waxy liquid (bulk) phase (**a**) and of the isolated solid phase (**b**) of zirconium *n*-butoxide

oxo-alkoxide species and other impurities, i.e., hydrolyzed species, there will be a need for alternative uniform structured zirconium precursors for reproducible preparation of materials. In this respect the precursors with propoxide ligands may be preferred above those with butoxide, since propanol solvent can be removed easier, i.e., the lower boiling point. It is important, however, also to remember that the resulting colloids are stabilized through interaction of the residual ligands with the solvent (MTSALs—micelles templated by self-assembly of ligands [22]), which favors in contrast application of longer-chain ligands.

Zirconium isopropoxide isopropanol solvate, $[Zr(O^iPr)_4(^iPrOH)]_2$ [15], is considered as a poor alternative as precursor since it is rather expensive and poorly soluble in parent alcohol and toluene. More interesting is the mixed ligand precursor, $[Zr(O^nPr)(O^iPr)_3(^iPrOH)]_2$ recently reported by Seisenbaeva et al. [17]. Both precursors have the dinuclear structure as depicted in Fig. 1d. As to the mixed ligand precursor, the *n*-propoxide ligands are in the position labelled with $OR_1$. The mixed ligand precursor has been prepared, according to the synthesis described above and in reference [17]. The yield, after the separation of three batches of crystals, of $[Zr(O^nPr)(O^iPr)_3(^iPrOH)]_2$ from 10 ml of zirconium *n*-propoxide was slightly higher compared to the route described in reference [17], e.g., 7.8 and 7.4 g. Main advantage of the presented synthesis route is the lower volume in the crystallization step.

The products of both routes were characterized by NMR and turned out to give spectra (Fig 2c) in accordance with the expected structure [17]. The triplets at 3.86 and 0.87 ppm and the sextet at 1.65 ppm are due to the bridging *n*-propoxide ligands (respectively, $OCH_2$, $CH_3$ and $CH_2$). While the septet at 4.28 ppm and the doublet at 1.18 ppm can be assigned to the *CH* and $CH_3$ of the terminal isopropoxide groups.

It was judged to be of interest to see if the solution that was removed from the last batch of crystals contained the same complexity as that found in zirconium *n*-propoxide. The solution separated from the third batch of crystals of $[Zr(O^nPr)(O^iPr)_3(^iPrOH)]_2$ was dried under vacuum. The spectrum of the obtained material is displayed in Fig. 2d. The main difference of the present spectrum with that obtained for $[Zr(O^nPr)(O^iPr)_3(^iPrOH)]_2$ can be seen in the signals between 3.8 and 4.5 ppm and the disappearance of the signal at 3.65 ppm. Assuming that the starting zirconium *n*-propoxide contained around ~80% $Zr(O^nPr)_4$ and ~20% of $Zr_3O(OR)_{10}$ and taking into account the yield of $[Zr(O^nPr)(O^iPr)_3(^iPrOH)]_2$ was ~90%, means that the majority of $Zr_3O(OR)_{10}$ has been converted into an oxo-ligand free product. The oxo-ligands supposedly have concentrated into poly-oxo-aggregates, $Zr_nO_{2n-x}(OPr)_{2x}$, as has been demonstrated for aluminium propoxide compounds [23]. This supposition is confirmed by slow solidification/gelation of the thus obtained residues in time (on rigorous protection from moisture).

The mass spectrometric analysis of $[Zr(O^nPr)(O^iPr)_3(^iPrOH)]_2$ showed a great number of signals between 450 and 600 m/z. The most dominant peaks at 532 (100%), 564 (~97%), and 593 (~55%) m/z can be assigned to $Zr_2(OR)_6$, $Zr_2(OR)_6(OCH_2)^+$, and $Zr_2(OR)_7$, respectively. Except for the signal at 817 m/z (<5%), there were no signals corresponding to a higher mass present. The latter originates supposedly from partial decomposition on evaporation as indicated by its low intensity.

The mass spectrometry data clearly shows that also in the gas phase $[Zr(O^nPr)(O^iPr)_3(^iPrOH)]_2$ is dimeric. This result is, in contrast with the mass spectrometry data for zirconium isopropoxide [9], where a significant amount of $Zr_4$ compounds were present, i.e., a lot of signals were obtained at higher masses. The fact that $[Zr(O^nPr)(O^iPr)_3(^iPrOH)]_2$ consists of dimeric species in the gas phase, strengthens that the precursor consists of one compound.

Besides the advantage of $[Zr(O^nPr)(O^iPr)_3(^iPrOH)]_2$ being a single compound precursor, i.e., in contrast to what has been shown for zirconium *n*-propoxide and *n*-butoxide, its physico-chemical properties are also very attractive. At room temperature the solubility is about 40 wt% in toluene and 30 wt% in isopropanol, compared to ~15 wt% in toluene and ~3% in isopropanol for zirconium isopropoxide.

### 3.2 Zirconium and hafnium alkoxide precursors modified by acac-ligands

The zirconium propoxide precursors utilized in this study, i.e., zirconium *n*-propoxide, isopropoxide, mixed ligand

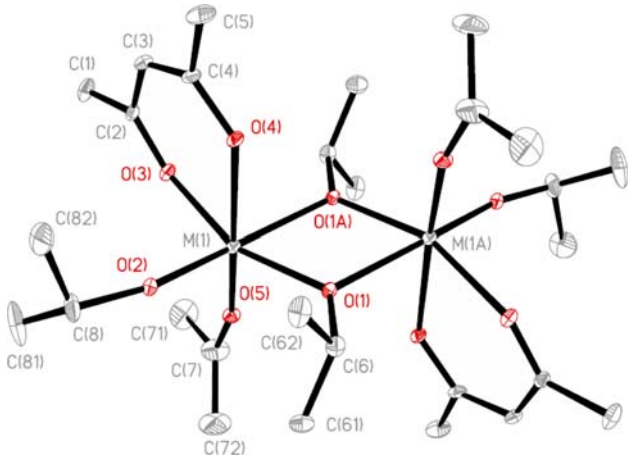


**Fig. 6** Molecular structure of $[M(O^iPr)_3(acac)]_2$, where M = Zr (**2**) or Hf (**4**)

compound, and hafnium isopropoxide and *n*-propoxide were modified with 1 mol equivalent of Hacac, in a manner analogous to one described in the experimental section for zirconium iso-propoxide. Only from isopropoxide solutions, X-ray quality single crystals could be obtained and characterized as $[M(O^iPr)_3(acac)]_2$, M = Zr(**2**), Hf(**4**) as is depicted in Fig. 6.

Structural analogs of compounds **2** and **4** have been reported earlier [24, 25]. They were obtained upon the modification of zirconium and hafnium isopropoxide with 1 mol equivalent of a bulky *β*-diketonate, 2,2,6,6,-tetramethylheptanedione (Hthd). The application of these compounds was proposed, however, for MOCVD (Metal Organic Chemical Vapor Deposition). The utilization of the bulky Hthd, as modifier for sol–gel applications is not considered attractive due to the large amount of carbon in the (rather expensive) bulky ligand that has to be removed during thermal treatment of the derived material. The bulky ligands in Hthd make it a stronger chelating ligand compared to Hacac. This effect can also be seen when the bond lengths of $[Zr(O^iPr)_3(thd)]_2$ are compared with that of **2**. From Table 3, the expected elongation of all the metal-oxygen bonds can clearly be seen and also the angle O(1)-M-(O1A) is significantly larger. This explains the acceleration of the hydrolysis-polycondensation process with formation of MTSALs on application of *β*-diketonates as modifying ligands [22].

$^1$H NMR spectrum obtained from freshly dissolved single crystals of **2** is relatively simple, containing sharp singlet at 5.60 and 1.97 ppm attributed to the *CH* and $CH_3$ of the acetylacetone, respectively, with an integration ratio of 1 to 6, and septets at 4.39 and 4.22 ppm, were assigned to the *CH* of the alkoxide ligands and overlapping doublets in the region between 1.0 and 1.3 ppm, identified as $CH_3$ signals of the alkoxide groups. On storage of solutions, the spectra start to reveal new signal, among which we could already, at the beginning of this study, clearly identify those of $Zr(acac)_4$.

For the samples where zirconium *n*-propoxide or mixed ligand propoxide was modified with 1 mol equivalent, only spectra with multiple signals could be obtained, indicating the formation of a mixture of compounds. However, the signal assigned to **2** could also be seen, indicating the formation of $[Zr(O^iPr)_3(acac)]_2$. We recently reported the formation of *β*-diketonate mono-substituted compounds from zirconium *n*-propoxide and mixed-ligand derivative, using Hthd [25]. The presence of the different compounds is probably one of the reasons why we did not succeed in the preparation of single-crystals in these systems. Another reason is the presence of *n*-propoxide ligands in these systems. These ligands make compounds well-soluble in hydrocarbons and difficult to crystallize.

The existence of other compounds formed upon modification with Hacac was already seen in the NMR data. An attempt was made to isolate the compound by modifying zirconium isopropoxide with 2 mol equivalents of Hacac. According to the literature, this would yield a disubstituted compound [24, 26, 27]. To our surprise, the crystals prepared as described above could be identified as $Zr(O^iPr)(acac)_3$ (**3**). This mono-nuclear compound, depicted in Fig. 7, has very poor stability. The decomposition of this compound was already observed during the single crystal diffraction experiments. A change in color and composition of the air tight sealed crystals was observed at the end of data collection (8–10 h after mounting the crystals). The two

**Table 3** Selected bond lengths and angles from the compounds **2**, **4**, $[Zr(thd)(O^iPr)_3]_2$ and $[Hf(thd)(O^iPr)_3]_2$

| | (**2**) | $[Zr(O^iPr)_3(thd)]_2$ | (**4**) | $[Hf(O^iPr)_3(thd)]_2$ |
|---|---|---|---|---|
| M–O(1) | 2.142(4) | 2.119 | 2.058(9) | 2.102 |
| M–O(1A) | 2.337(5) | 2.219 | 2.147(9) | 2.192 |
| M–O(2) | 2.022(4) | 1.944 | 1.858(10) | 1.953 |
| M–O(3) | 2.187(5) | 2.153 | 2.096(10) | 2.102 |
| M–O(4) | 2.264(4) | 2.190 | 2.164(10) | 2.169 |
| M–O(5) | 1.962(4) | 1.931 | 1.906(10) | 1.927 |
| M(1)–M(1A) | 3.598(6) | 3.508 | 3.403(2) | 3.476 |
| O(1)–M–(O1A) | 73.19(14) | 72.07 | 71.9(4) | 72.0 |

The data from the latter two compounds was taken from ref. [24]

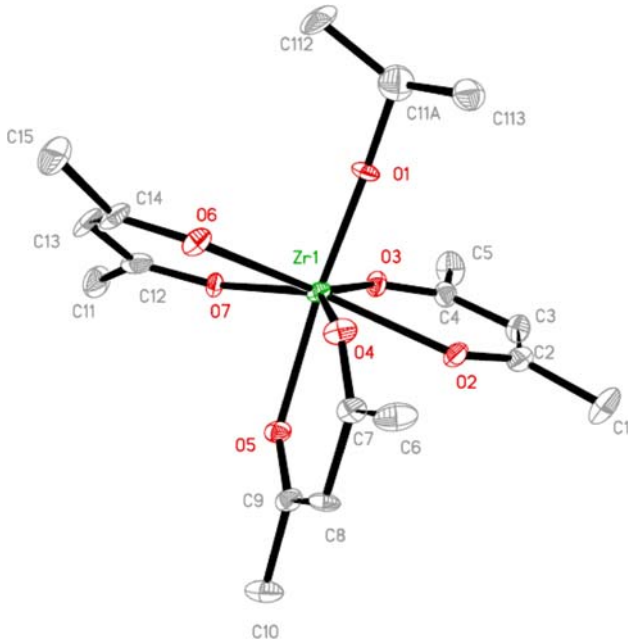


**Fig. 7** Molecular structure of $[Zr(O^iPr)(acac)_3]$ (**3**)

metal-oxygen bond lengths of the acac ligand in **3** are almost identical. The absence of trans-stabilization in compound **3** probably explains the poor stability of the compound, and the absence of trans-stabilization is probably the reason why mononuclear disubstituted derivatives (otherwise well-known for asymmetrically bound ligands such as ketoesterates [28, 29]) with $\beta$-diketonate can not be obtained. The NMR spectrum of 3 (5.56 singlet and 1.95 singlet corresponding to *CH* and $CH_3$ of the acetylacetone, respectively and a poorly resolved septet at 4.25 ppm together with a doublet at 0.98 ppm, *CH* and $CH_3$ of the alkoxide) is always contaminated by the signals originating from $Zr(acac)_4$, indicating facile transformation into this species.

The existence of the tri-substituted compound was also evaluated for the zirconium mixed-ligand precursor. After the addition of 2 mol equivalents of Hacac to the mixed-ligand precursor solution, the initial NMR spectra recorded 10 min after sample preparation showed multiple peaks around 5.5 ppm. The largest signal in the spectrum is assigned to Zr(acac)4, since only this peak remained after 16 h. The two minor peaks are attributed to the intermediate tri-substituted and the mono-substituted structure. The presence and disappearance after 16 h of peaks assigned to normal and isopropoxide $CH_3$ groups lend support to the conclusion to that the tri-substituted precursor is initially formed in this system. After 16 h, the spectra changed with respect to the position of the peaks corresponding to the alkoxide groups in bridging positions. The presence of various species is also one of the reasons why the preparation of single crystals from these systems is hindered.

After isolation and characterization of the tri-substituted compound **3**, NMR experiments were conducted to seek for the presence of compounds supposed to be formed upon modification with 0.5 and 2 mol equivalents of Hacac as proposed in literature. For samples of zirconium isopropoxide modified with 0.5 mol equivalent of Hacac, formation of only mono-substituted and unmodified precursors was observed. For zirconium isopropoxide with more than 1 mol equivalent, the only signals present in the spectra were those assigned to **2**, **3** and $Zr(acac)_4$. Hence, we consider that no compounds other than **3** are formed upon modification of zirconium propoxides with Hacac.

It is thus clear that the nature of the heteroleptic intermediates of different zirconium propoxides characterized in this study is not in agreement with the mechanism and structures proposed in literature. Upon addition of up to 1 mol equivalent Hacac, the most stable intermediate $[Zr(O^iPr)_3(acac)]_2$ is formed. When additional Hacac is added, the $[Zr(O^iPr)_3(acac)]_2$ structure is destabilized leading to the presence of the initial precursor and unstable $Zr(O^iPr)(acac)_3$. Spontaneous and rapid rearrangement of $Zr(O^iPr)(acac)_3$ to stable $Zr(acac)_4$ occurs at room temperature.

We have also attempted to get more insight in the formed intermediate structures of the zirconium *n*-butoxide system. A sample with 1 equivalent mol of Hacac was prepared and subsequently dried under vacuum. The $^1H$ NMR spectrum of this compound showed greater similarities with that obtained for zirconium *n*-propoxide with 1 equivalent mol of Hacac, i.e., the same signals were observed between 5 and 6 ppm. The attempts to isolate single crystals were, as could be expected, not successful. The removal of the parent solvents is even more complicated for *n*-butanol compared to that of *n*-propanol due to the higher boiling point of *n*-butanol. Despite the limited data, we do not expect that the heteroleptic intermediates differ from those that were obtained for the zirconium isopropoxide systems. It is then very unlikely that the commercially available di-acac substituted zirconium *n*-butoxide precursor exists; it is probably a complex mixture of unmodified, mono-, tri-, and tetra-substituted compounds as we have demonstrated for the thd-modified derivatives [25]. The behavior of the hafnium analogs turned out to be very analogous with slightly modified solution stability that was noticeably higher for monosubstituted compound $[Hf(O^iPr)_3(acac)]_2$ (**4**) and lower for the tris-substituted analog, which facile decomposition precluded its isolation in a pure form.

It was important to characterize quantitatively the stability of the obtained compounds. It has already been mentioned above that the stability of **3** is very low. Therefore, the stability experiments were performed on the monosubstituted compounds, i.e., **2** and **4**. Batches of

crystals of these compounds were synthesized. During drying, a color change was occasionally observed, i.e., the initial white crystals turned yellow. This suggests a change in composition; the batches in which this occurred were not used for further experiments. NMR samples with various concentrations of **2** or **4** were prepared. After the addition of the solvent, $CDCl_3$, the NMR tubes were rapidly placed in the NMR spectrometer. A spectrum was recorded as soon as the sample had reached the measuring temperature of 243 K. After the measurements, the samples were taken out of the spectrometer and stored on the lab bench (temperature 296.3 K) till the next measurement. The region between 5 and 6 ppm, corresponding to the signal of the *CH* of the acetylacetone ligand, was used for determining the concentration. The surface area of the signal assigned to **2** or **4** was normalized by the total area between 5 and 6 ppm. The change in composition was monitored by repeating the described procedure various times. For the interpretation of the data, we assumed that the initially dissolved product was purely **2** or **4**. The results of experiments are depicted in Fig. 8.

The general trend for all experiments, depicted in Fig. 7, is a strong decrease in the concentration of the initial species in time. This is also what one would expect on the basis of the proposed mechanism for stabilization and destabilization. Compounds **2** and **4** rearrange through the formation of a tri-substituted and finally the formation of unreactive tetra-substituted compounds. The driving force for the observed decreased concentration of **2** or **4** is thus, the formation of tetra-substituted compounds. An important factor that might influence the transformation towards $M(acac)_4$ is the facilitating effect of the residual alcohol observed earlier for rearrangement of alkoxide $\beta$-diketonate derivatives [30]. The presence of traces of alcohol can not be excluded, and the possible effect should be taken in consideration. This latter effect makes the quantitative interpretation of the data not completely reliable. However, further analysis of the data is possible and indicates that the reaction order of the rearrangement of compounds **2** and **4** is between 1 and 2, which is logical in the view of the need for intermolecular ligand transfer for this transformation. This quick change in concentrations of the precursor species in time causes problems in attempts to apply the alkoxide $\beta$-diketonate derivatives as precursors for the synthesis of materials with reproducible porosity [31].

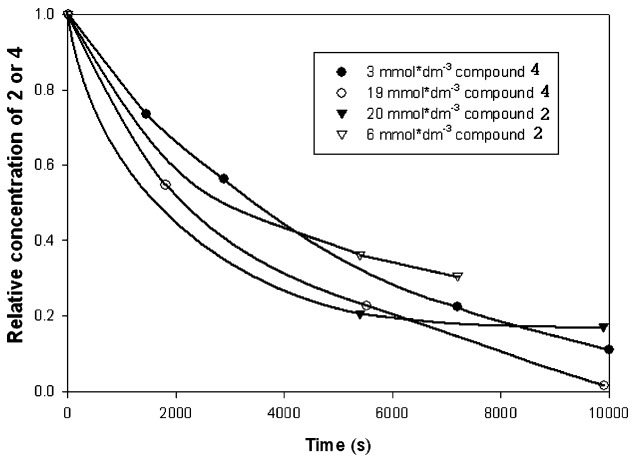


**Fig. 8** The decrease in the concentrations of **2** and **4** in time determined by $^1$H NMR

It is evident that the study of modification of zirconium or hafnium alkoxides with acetylacetone cannot be carried out using EXAFS or XANES spectroscopy: the registration of a spectrum using these techniques requires 1 h or 20–30 min, respectively, i.e., a time span associated with already rather deep transformation in the studied systems, transforming even the possible individual intermediates into complex mixtures.

## 4 Conclusions

The presence of $Zr_3O(OR)_{10}$ core containing species in zirconium *n*-propoxide and *n*-butoxide has been demonstrated on the basis of data of X-ray single crystal, NMR and mass spectrometry. The commercially available zirconium *n*-propoxide and *n*-butoxide products contain possibly up to $\sim$20 and $\sim$35% of $Zr_3O(OR)_{10}$ derived species, respectively. This impurity is most probably resulting from the conditions of synthesis, applying zirconium chloride complexes and alcohol in combination with an organic base. The substitution reaction is carried on under reflux, which is facilitating in such systems the non-hydrolytic formation of oxo-species [32].

The new preparation route of $[Zr(O^nPr)(O^iPr)_3(^iPrOH)]_2$ turns out to be attractive. The obtained compound can be considered as an alternative for expensive zirconium isopropoxide and the multi components present in zirconium *n*-propoxide and *n*-butoxide. The solubility of $[Zr(O^nPr)(O^iPr)_3(^iPrOH)]_2$ in propanol is another great advantage over zirconium isopropoxide.

Modification of zirconium or hafnium alkoxides with Hacac leads to either monosubstituted derivatives, $[M(OR)_3(acac)]_2$, with hexacoordinated metal atoms or trisubstituted ones, $[M(OR)(acac)_3]$, containing heptacoordinated metal atoms. No disubstituted complexes could be isolated with propoxide or n-butoxide ligands. The alkoxide $\beta$-diketonate derivatives of zirconium and hafnium are instable in time and transform in solution into unreactive and hydrolysis insensitive $M(acac)_4$. Relatively high speed of this transformation makes application of slow data-accumulating techniques such as EXAFS or XANES, inapplicable for the studies of such systems.

## 5 Supplementary

Full crystallographic details have been deposited with the Cambridge Crystallographic Data Centre. Copies of the data can be obtained free of charge on request from the CCDC, 12 Union Road, Cambridge CB2 1EZ, UK (fax: +44 1233 336033; e-mail: deposit@ccdc.cam.ac.uk or http://www.ccdc.cam.ac.uk/conts/retrieving.html) quoting the deposition numbers **721855** (**1**), **237185** (**2**), **237186** (**3**), and **721856** (**4**).

Variable temperature $^{1}$H NMR data for different fractions of "Zr(OnPr)4" and the compound 1 are available on request from the authors.

**Acknowledgments** The authors are very grateful to Rolf Andersson and Dr. Corine Sandström for the assistance with the NMR analysis and to Suresh Gohil for performing the mass spectrometry experiments. Dr. ir. Nieck E. Benes (University of Eindhoven) is kindly acknowledged for the scientific discussions. We thank the Swedish Research Council (Vetenskapsrådet) and the Dutch Economy-Ecology-Technology (EET) program for support of this research.

## References

1. Benfer S, Popp U, Richter H, Siewert C, Tomandl G (2001) Separ Purif Tech 22–23:231. doi:10.1016/S1383-5866(00)00133-7
2. Vacassy RJ, Guizard C, Palmeri J, Cot L (1998) NanoStructured Mater 10:77. doi:10.1016/S0965-9773(98)00022-1
3. Xia CR, Cao HQ, Wang H, Yang PH, Meng GY, Peng DK (1999) J Membr Sci 162:181. doi:10.1016/S0376-7388(99)00137-4
4. Haruta M, Kobayashi T, Sano H, Yamada N (1987) Chem Lett 829:405. doi:10.1246/cl.1987.405
5. Knell A, Barnickel P, Baiker A, Wokaun A (1992) J Catal 137:306. doi:10.1016/0021-9517(92)90159-F
6. Hoffman S, Klee M, Waser R (1995) Integr Ferroelectr 10:155. doi:10.1080/10584589508012273
7. Klee M, Mackens U, Hermann W, Bathelt E (1995) Integr Ferroelectr 11:247. doi:10.1080/10584589508013596
8. Day VW, Klemperer WG, Pafford MM (2001) Inorg Chem 40:5738. doi:10.1021/ic010776g
9. Turevskaya EP, Kozlova NI, Turova NY, Belokon AI, Berdyev DV, Kessler VG, Grishin YK (1995) Bull Russ Acad Sci (Russ) Chem (Kyoto):752
10. Kanazhevskii VV, Shmachkova VP, Kotsarenko NS, Kolomiichuk VN, Kochubei DI (2006) J Struct Chem 47:453. doi:10.1007/s10947-006-0322-8
11. Bauer M, Gastl C, Köppl C, Kickelbick G, Bertagnolli H (2006) Monatsh Chem 137:567. doi:10.1007/s00706-006-0450-z
12. Bauer M, Müller S, Kickelbick G, Bertagnolli H (2007) N J Chem 31:1950. doi:10.1039/b707079a
13. Caughlan CN, Smith HS, Katz W, Hodgson W, Crowe RW (1951) J Am Chem Soc 73:5652. doi:10.1021/ja01156a046
14. Russo WR, Nelson WH (1970) J Am Chem Soc 92:1521. doi:10.1021/ja00709a013
15. Vaartstra BA, Huffman JC, Gradeff PS, Hubert-Pfalzgraf LG, Daran J-C, Parraud S, Yunlu K, Caulton KG (1990) Inorg Chem 29:3126. doi:10.1021/ic00342a014
16. Boyle TJ, Gallegos JJ, Pedrotty DM, Mechenbier ER, Scott BL (1999) J Coord Chem 47:155. doi:10.1080/00958979908024550
17. Seisenbaeva GA, Gohil S, Kessler VG (2004) J Mater Chem 14(21):3177. doi:10.1039/b404303k
18. Spijksma GI, Bouwmeester HJM, Blank DHA, Kessler VG (2004) Chem Comm 1874
19. SHELXTL-NT program manual, Bruker AXS 1998
20. Veith M, Mathur S, Mathur C, Huch V (1997) J Chem Soc, Dalton Trans 2101. doi:10.1039/a700833c
21. Hagfeldt C, Kessler V, Persson I (2004) Dalton Trans 2142. doi:10.1039/b402804j
22. Kessler VG, Spijksma GI, Seisenbaeva GA, Håkansson S, Blank DHA, Bouwmeester HJM (2006) Sol-Gel Sci Tech 42:163
23. Starikova ZA, Kessler VG, Turova NY, Tcheboukov DE, Suslova EV, Seisenbaeva GA, Yanovsky AI (2004) Polyhedron 23:109. doi:10.1016/j.poly.2003.09.031
24. Fleeting KA, O'Brien P, Otway DJ, White AJP, Williams DJ, Jones AC (1999) Inorg Chem 38:1432–1437. doi:10.1021/ic980690w
25. Spijksma GI, Bouwmeester HJM, Blank DHA, Fischer A, Henry M, Kessler VG (2006) Inorg Chem 44:9938
26. Jones AC, Leedham TJ, Wright PJ, Crosbie MJ, Lane PA, Williams DJ, Fleeting KA, Otway DJ, O'Brien P (1998) Chem Vap Deposition 4:46. doi:10.1002/(SICI)1521-3862(199803)04:02<46::AID-CVDE46>3.0.CO;2-1
27. Jones AC, Leedham TJ, Wright PJ, Crosbie MJ, Williams DJ, Fleeting KA, Davies HO, Otway DJ, O'Brien P (1998) Chem Vap Deposition 4:197. doi:10.1002/(SICI)1521-3862(199810)04:05<197::AID-CVDE197>3.3.CO;2-U
28. Patil U, Winter M, Becker HW, Devi A (2003) J Mater Chem 13:2177–2184. doi:10.1039/b304419j
29. Baunemann A, Thomas R, Becker R, Winter M, Fischer RA, Ehrhart P, Waser R, Devi A (2004) Chem Commun (Camb) 1610–1611. doi:10.1039/b405015k
30. Kessler VG, Gohil S, Parola S (2003) Dalton Trans 544. doi:10.1039/b206662a
31. Kreiter R, Rietkerk MDA, Bonekamp BC, van Veen HM, Kessler VG, Vente JFJ (2008) Sol–Gel Sci Tech (Paris) 48:203
32. Vioux A (1997) Chem Mater 9:2292. doi:10.1021/cm970322a
33. Turova NY, Turevskaya EP, Kessler VG, Yanovskaya MI (2002) The chemistry of metal alkoxides. Kluwer AP, Dordrecht